Table of Contents

Methods

^{1}H NMR and ^{31}P NMR-spectra were obtained using a Bruker Ascend™ 400MHz spectrometer.

Infra-red spectra were measured using a Bruker Alpha FTIR spectrometer with a platinum ATR module.

UV/Vis absorption spectroscopy was performed on a Cary 5000 UV/VIS NIR spectrophotometer.

Electrospray ionisation mass spectrometry (ESI-MS) was performed on a *Bruker MicroTOF spectrometer.*

CHN microanalysis was carried out using an Exeter Analytical CE-440 Elemental Analyser.

Thermogravimetric analysis (TGA) was carried out using a TA Instruments Discovery TGA. Samples were heated on HT-platinum pans from 25-700°C under air at 10°C/min.

Dynamic Light Scattering (DLS) measurements were acquired using a Malvern Instrument Nano-ZS Zetasizer at room temperature.

Cryo-TEM samples were prepared and imaged using a Gatan CP3 cryoplunge and a JEOL 2100 Plus operating at 200 kV. The sample was deposited (3 µL) onto a graphene oxide / holey carbon copper grid, held in tweezers (25 °C, 80% humidity), and blotted (1.5 s), before plunging into liquid ethane (-172 °C) to vitrify. The sample was maintained under liquid nitrogen (-196 °C) during transfer (Gatan 926 cryo sample holder) to the TEM, with the temperature held around –176 °C throughout imaging with a Gatan (Smartset model 900) cold stage controller. Images were recorded (Gatan Ultrascan 100XP camera), with a nominal underfocus value of 3-5 µm and a 60 µm objective aperture to enhance phase contrast.

TEM experiments were run by Dr. Michael Fay at the Nanoscale and Microscale Research Centre (University of Nottingham) on a JEOL 2100F operating at 200 kV, equipped with a Gatan Orius camera for imaging and an Oxford Instruments XMax 80 for EDX analysis. Samples (0.5 mg in 5 mL DMF) were dispersed onto graphene oxide on holey carbon film supports (EM Resolutions). Particle size analysis was performed using a python script based on the particle analysis module of the SimpliPyTEM package.[1]

Electrochemical measurements were performed on CHI600e and CHI450c (CH Instruments) workstations. CV experiments under non-aqueous conditions were performed using a three-electrode arrangement: working electrode (glassy carbon, d= 3mm or gold, d= 2 mm), reference electrode (Ag wire) and a counter electrode (Pt wire) in $TBAPF_6$ (0.1 M) as the supporting electrolyte in dry DMF. Experiments under aqueous conditions were performed using a working electrode (glassy carbon, d= 3mm or gold, d= 2 mm), reference electrode (AgCl│Ag) and a counter electrode (Pt wire) in H_3PO_4 (0.1 M) as the supporting electrolyte. For surface-confined electrochemistry experiments, the 2 mm diameter gold disk electrode was prepared by polishing on porous neoprene with 0.05 µm, 0.3 µm and 1 µm alumina before sonicating in Milli-Q water for 1 min. The electrode was then rinsed with Milli-Q water

and then immersed in piranha solution (30% H_2O_2–conc. H_2SO_4, 1:3 v/v) for 10 min, before sonicating in Milli-Q water again for 1 min and rinsed with Milli-Q water. The electrode was then cycled in a 0.5 M H_2SO_4 solution from -0.1 to 1.2 V for 25 cycles at 100 mVs^{-1}, before finally rinsing with Milli-Q. For the deposition of a monolayer of molecular POMs: the electrode was then rinsed with DMF before immersing in a stirred 1 mM solution of POM in DMF for 24 h. The electrode was rinsed thoroughly with DMF before it was placed in fresh electrolyte solution (0.1 M $TBAPF_6$ in DMF) for the CV experiments. For the deposition of POM micelles: the clean electrode was immersed in a stirred 1.4 mM solution of POM in 9:1 H_2O-DMF (v/v) for 24 h. The electrode was rinsed thoroughly with Milli-Q before it was placed in fresh electrolyte solution (0.1 M H_3PO_4) for the CV experiments. All solutions were purged with nitrogen for 10 mins and kept under a positive pressure of nitrogen for the duration of the experiment.

AFM samples were mounted into an Asylum Research Cypher-S AFM system set up with a silicon cantilever tip (Multi75AL-G silicon cantilever from Budget Sensors) and imaged in AC mode AFM with the cantilevers driven just off resonance frequency. The Au/mica substrates were submerged in either a solution of **4** (0.25 mM in DMF) or **4** micelles (1.4 mM in 9:1 H_2O-DMF v/v), held by tweezers at one corner. The substrates were then rinsed thoroughly with DMF and then Milli-Q before being allowed to dry in air.

Syntheses and Materials

All reagents were obtained from commercial sources and were used without further purification.

Synthesis of K_{10}-[$P_2W_{17}O_{61}$] {P_2W_{17}}

K_{10}-[$P_2W_{17}O_{61}$] and its precursor, K_6-[$P_2W_{18}O_{62}$], were synthesised according to procedures in literature.[3, 4]

Synthesis of TPY

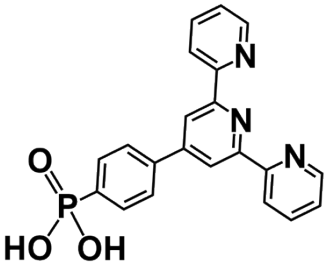

TPY was prepared according to our previously reported procedure.[1]

Synthesis of $C_{11}SH$

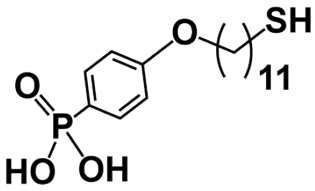

$C_{11}SH$ was prepared and supplied by Dr Carmen Martin-Gandul according to our previously reported procedure.[2]

Synthesis of asymmetric POM hybrid **(4),**

$K_5(C_2H_8N)[P_2W_{17}O_{57}\{(PO_3C_{21}H_{14}N_3)(PO_4C_{17}H_{26}SH)\}]$

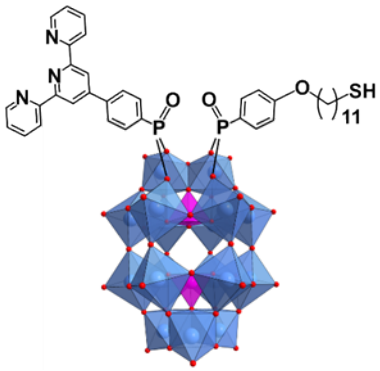

K_{10}-$[P_2W_{17}O_{61}]$ (2 g, 0.439 mmol), **TPY** (0.171 g, 0.439 mmol), **C_{11}SH** (0.158 g, 0.439 mmol), and KCl (0.65 g, 8.72 mmol) were suspended in DMF (35 mL) and stirred. 12M HCl (256 µL, 3.07 mmol) was added dropwise to the solution whilst stirring, and the mixture was heated to 85°C for 19 h. The mixture was allowed to cool to RT before filtering. An excess of ether was added (75 mL) to give a milky yellow solution, which was centrifuged to give a beige precipitate in a yellow supernatant. The solvent was decanted and the process of sonicating the precipitate in ether, centrifuging and decanting was repeated until the precipitate resembled a free-flowing beige powder. The solid was then sonicated in acetonitrile (10 mL) and centrifuged to separate an

insoluble pale green-blue solid. The yellow supernatant was decanted and ether was added (20 mL) to it to precipitate a pale orange-beige solid and leave a pale yellow supernatant. The process of: re-dissolving in acetonitrile and centrifuging to remove any insoluble **2**, followed by re-precipitating **4** from the supernatant with ether, was repeated until no **2** or **3** was visible in the ^{31}P and ^{1}H NMR. The solid was collected by centrifugation, sonicated in ether and centrifuged again. The solvent was decanted and the solid was dried in air with gentle heating to yield **4** as an light orange solid (416 mg, 19%).

^{1}H NMR (400.1 MHz, DMSO-d_6) δ = 8.84-8.65 (m, 6H; Ar-H), 8.26-8.16 (m, 2H; Ar-H), 8.16 (br, 2H; N**H$_2$**$(CH_3)_2^+$), 8.08-8.01 (m, 2H; Ar-H), 8.01-7.96 (m, 2H; Ar-H), 7.94-7.97 (m, 2H; Ar-H), 7.56-7.50 (m, 2H; Ar-H), 7.04-6.98 (m, 2H; Ar-H), 4.07-3.97 (m, 2H; O-C**H$_2$**), 2.55 (s, 6H; $NH_2(CH_3)_2^+$), 1.78-1.67 (m, 2H; C**H$_2$**-SH), 1.66-1.19 (m, 18H; -CH_2-) ppm; **^{31}P NMR** (162 MHz, DMSO-d_6) δ= 16.72, 13.41, -11.33, -12.95 ppm; **IR** (ATR): 424 (s), 471 (s), 527 (s), 568 (s), 578 (s), 595 (s), 729 (br, vs), 764 (br, vs), 908 (s), 953 (s), 1087 (s), 1134 (w), 1253 (w), 1295 (w), 1391 (w), 1414 (w), 1465 (m), 1504 (w), 1531 (w), 1597 (m), 1651 (w), 2852 (m), 2927 (m) cm^{-1}; **Elemental Analysis:** calc (%) for $K_5P_4W_{17}O_{64}C_{40}H_{49}N_4S_1$: C 9.45, H 0.97, N 1.10, found: C 9.47, H 1.21, N 0.78; **TGA Analysis:** Step transition (234.0 to 301.5°C) wt loss of 1.260 % = loss of 1 $C_2H_8N^+$ (DMA^+) (calc= 0.906 %); **UV/Vis (DMF)**: λ_{max} (ε, $mol^{-1}Lcm^{-1}$) = 276 (88,100), 315 (38,100) nm.

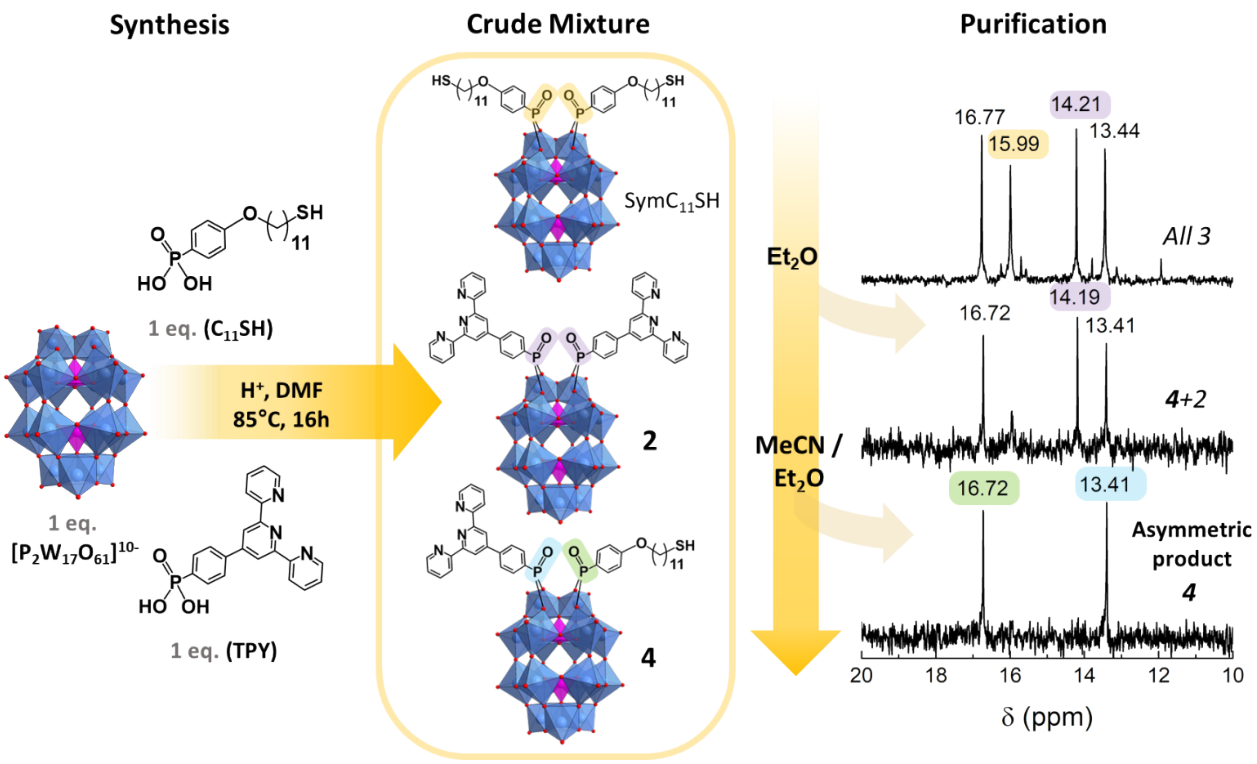

Figure S1. Synthesis and purification of the asymmetric hybrid-POM, **4**, and the symmetric by-products, **2** and **3**, illustrating the purification process. ^{31}P NMR of the reaction mixture in DMSO-d_6 is shown on the right, taken after each purification step (top: crude; middle **4** + **2**; bottom: **4** only). Chemical shifts corresponding to each product are colour coded as shown (note that for simplicity, only the positive chemical shift region for the organophosphonate ^{31}P nuclei is presented here). Colour code: blue polyhedra = {WO_6}, pink polyhedra = {PO_4}, red spheres = oxygen. Cations and solvent molecules are omitted for clarity.

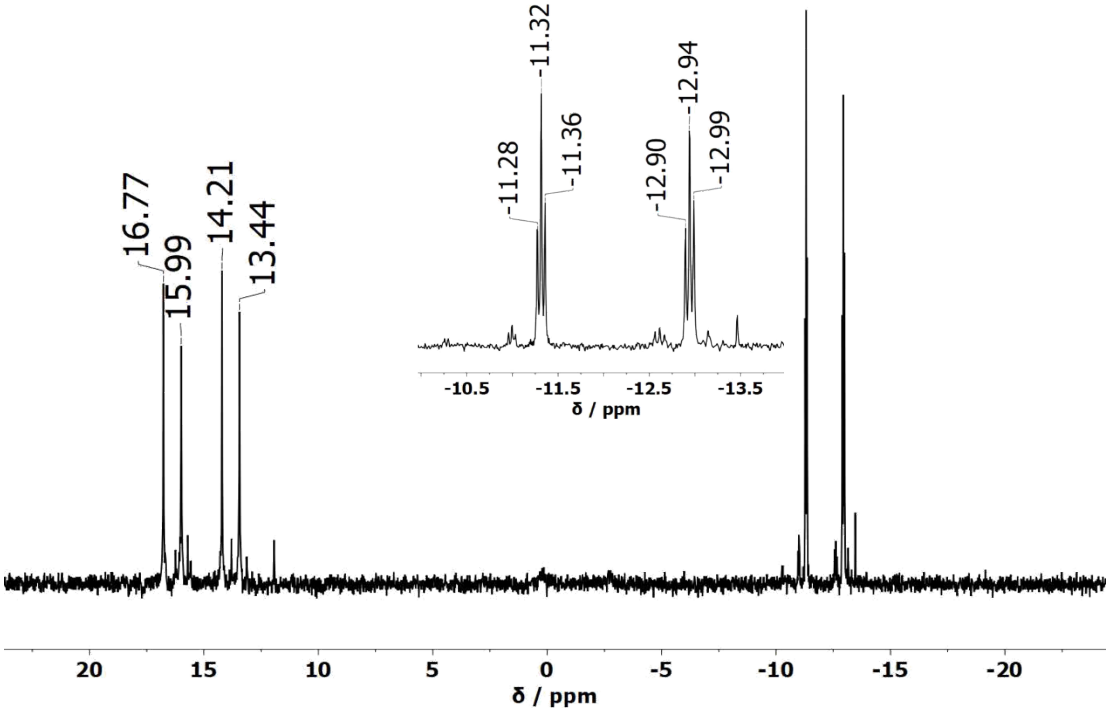

Figure S2. ^{31}P NMR of the crude mixture in the synthesis of **4** in DMSO-d_6. Inset shows an expansion of the peaks in the negative spectral region.

Targeted synthesis of symmetric hybrid **2**

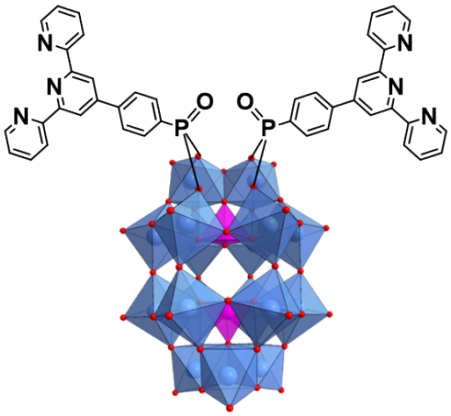

$(C_2H_8N)_6[P_2W_{17}O_{57}\{(PO_3C_{21}H_{14}N_3)_2\}]$

The symmetric TPY hybrid POM, **2**, was synthesised and characterised according to the methods described in our previous work.[1]

Targeted synthesis of symmetric hybrid **3**

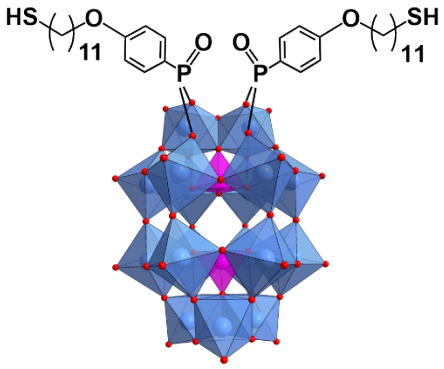

$K_3(C_2H_8N)_3[P_2W_{17}O_{57}\{(PO_4C_{17}H_{26}SH)_2\}]$

K_{10}-$[P_2W_{17}O_{61}]$ (0.25 g, 0.055 mmol), **C_{11}SH** (40 mg, 0.11 mmol), and KCl (82 mg, 1.1 mmol) were suspended in CH_3CN-DMF (1:1 v/v, 10 mL) and stirred. 12M HCl (37 µL, 0.44 mmol) was added dropwise to the solution whilst stirring, and the mixture was heated to 80°C for 20 h. The mixture was allowed to cool to RT before filtering. The solvent was reduced *in vacuo* to ~5 mL before an excess of ether was added (35 mL) to give a milky yellow solution, which was centrifuged to give a dark orange oil in a clear, colourless supernatant. The solvent was decanted and the process of sonicating the oily residue in ether, centrifuging and decanting was repeated until the precipitate resembled a free-flowing, dark orange powder. Finally, the solid was dried in air with gentle heating to yield **4** as a dark orange solid (175 mg, 64%).

^{1}H NMR (400.1 MHz, DMSO-d_6) δ = 8.19 (br, 6H; N**H_2**$(CH_3)_2^+$), 7.88 (dd, *J* = 13.5, 8.6 Hz, 4H; Ar-H), 6.99 (dd, *J* = 8.9, 3.3 Hz, 4H; Ar-H), 4.03 (t, *J* = 6.5 Hz, 4H; O-C**H_2**), 2.55 (t, *J* = 5.5 Hz, 18H; NH_2(C**H_3**$)_2^+$), 2.11 (t, *J* = 8.9, 2H; -S**H**), 1.78-1.66 (m, 4H; C**H_2**-SH), 1.46-1.20 (m, 32H; -CH_2-) ppm; **^{31}P NMR** (162 MHz, DMSO-d_6) δ= 15.94, -11.37, -12.99 ppm; **IR** (ATR): 424 (s), 471 (s), 525 (s), 566 (s), 593 (s), 729 (br, vs), 906 (s), 953 (s), 1085 (s), 1134 (w), 1183 (w), 1253 (w), 1292 (w), 1385 (w), 1414 (w), 1437 (w), 1463 (m), 1504 (w), 1568 (w), 1597 (m), 1651 (w), 2850 (m), 2922 (m) cm^{-1};

Preparation of **4-AuNPs**

The procedure reported by Martin *et al.* was adapted for the preparation of **4**-stabilised AuNPs.[1] Assuming ~400 POMs are needed per AuNP as determined by Martin *et al.,* **4** was used in approximately 20 times excess of the AuNPs.

4 (10 mg, 1.97 μmol) was dissolved in CH_3CN (2 mL) before a solution of citrate-stabilised AuNPs in water (10 nm, Sigma Aldrich, 25 mL, OD 1, ~6.0^{12} particles/mL) was added to it whilst stirring. The solution was stirred at RT in the dark for 2 days. The solution was centrifuged, and the supernatant was decanted from a small amount of insoluble material. The solvent was concentrated by removal in *vacuo* to ~ 1-2 mL, before an excess of MeOH was then added (~40 mL). The solution was centrifuged for 15 mins at 8000 rpm and the supernatant was decanted from a dark red-black precipitate. The precipitate was washed with MeOH-CH_3CN (1:1 v/v, 3 mL) three times and then once with ether (3 mL), collecting it each time by centrifugation (10 mins at 8000 rpm) and decanting the supernatant. Finally, the solid was allowed to dry in air to yield **4-NPs** as a dark red solid (0.5 mg).

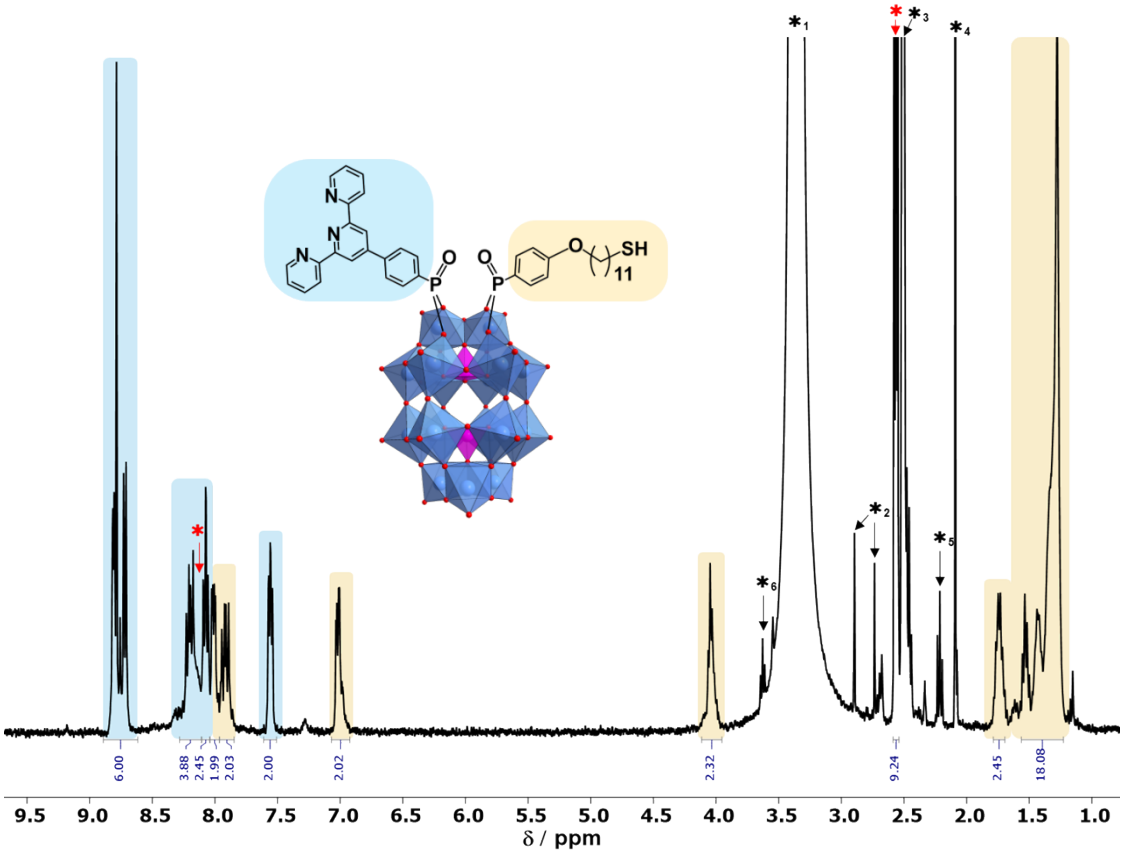

NMR Characterisation

Figure S3. ^{1}H NMR of **4** in DMSO-d_6 showing the assignment of signals to each ligand: yellow = *$C_{11}SH$*, blue = *TPY*. Red asterisks indicate DMA (C_2H_8N+) cation signals, and black asterisks indicate impurities: 1= H_2O, 2= DMF, 3= DMSO, 4 = CH_3CN, 5/6 = α-carbon hydrogen of thiol aerobic oxidation products (RSO_2H/RSO_3H)

Mass Spectrometry

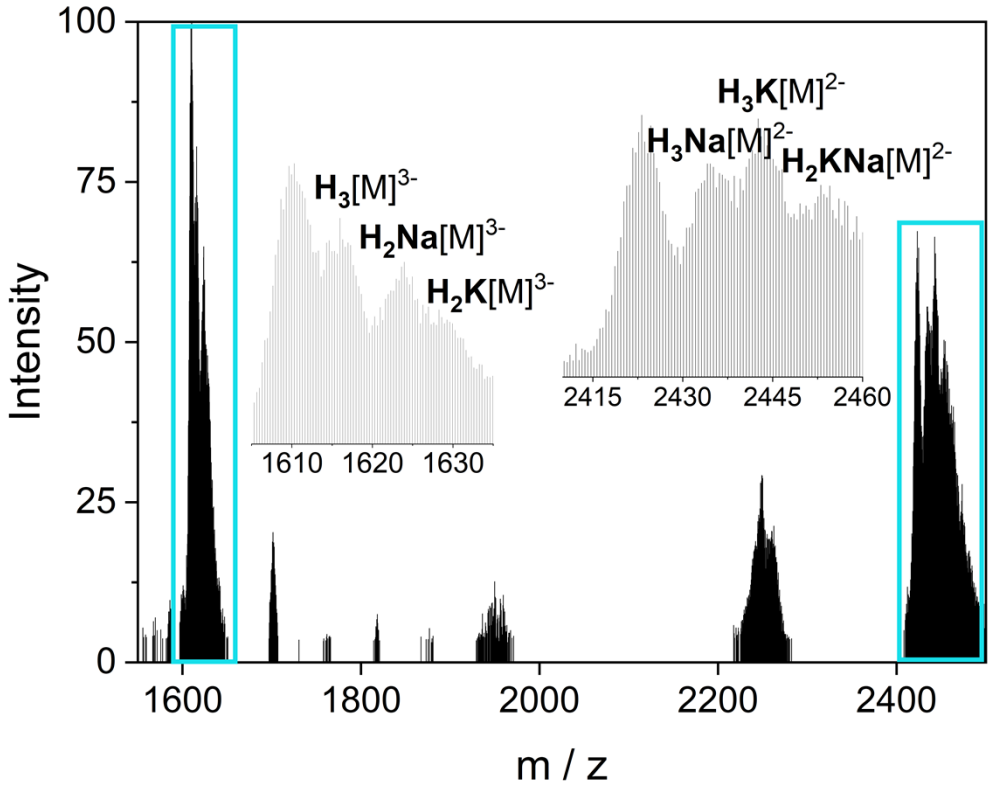

Figure S4. Negative mode ESI mass spectrum of **4** in acetonitrile. [M] = $[P_2W_{17}O_{57}\{(PO_3C_{21}H_{14}N_3)(PO_4C_{17}H_{26}SH)\}]^{6-}$.

Assignment	z	m/z (obs.)	m/z (calc.)
$\mathbf{H_3}[P_2W_{17}O_{61}(POC_{21}H_{14}N_3)(PO_2C_{24}H_{41})]$	3-	1615.9616	1615.9964
$\mathbf{H_2Na}[P_2W_{17}O_{61}(POC_{21}H_{14}N_3)(PO_2C_{24}H_{41})]$	3-	1623.2820	1623.3237
$\mathbf{HNa_2}[P_2W_{17}O_{61}(POC_{21}H_{14}N_3)(PO_2C_{24}H_{41})]$	3-	1628.5929	1628.6483
$\mathbf{H_2Na_2}[P_2W_{17}O_{61}(POC_{21}H_{14}N_3)(PO_2C_{24}H_{41})]$	2-	2435.6213	2435.4894
$\mathbf{HNa_3}[P_2W_{17}O_{61}(POC_{21}H_{14}N_3)(PO_2C_{24}H_{41})]$	2-	2443.5988	2443.4764
$\mathbf{Na_4}[P_2W_{17}O_{61}(POC_{21}H_{14}N_3)(PO_2C_{24}H_{41})]$	2-	2454.5525	2454.4674

Table S1. Observed and calculated m/z values and selected peak assignments for **4**.

FTIR Analysis

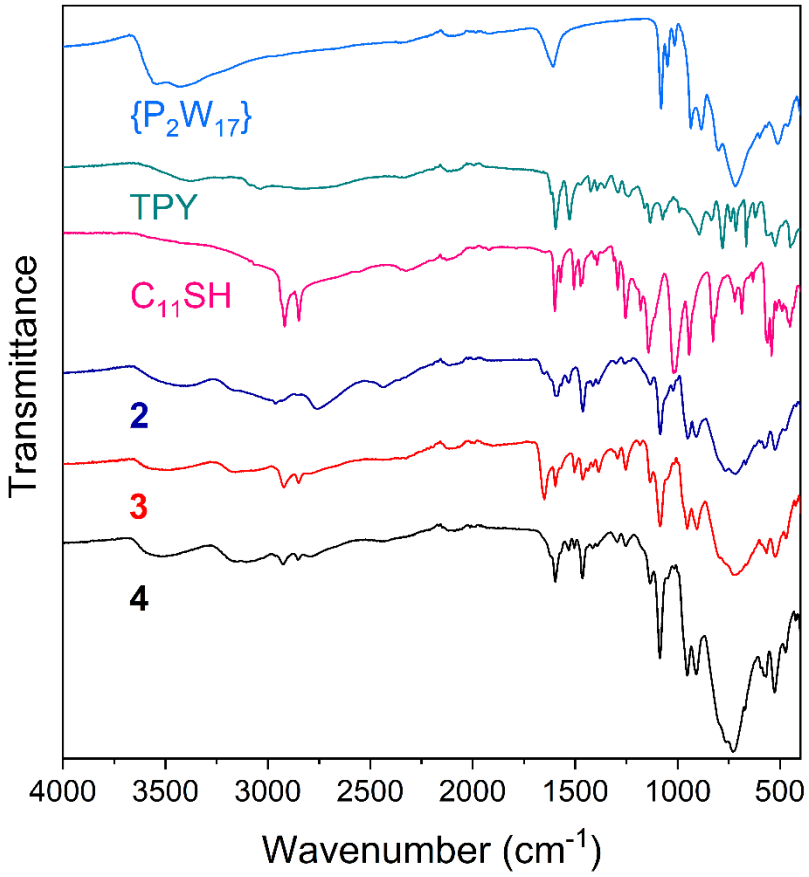

Figure S5. Comparison of ATR IR spectra of **4,** K_{10}-[$P_2W_{17}O_{61}$] {P_2W_{17}}, ligands **TPY** & **C_{11}SH**, &

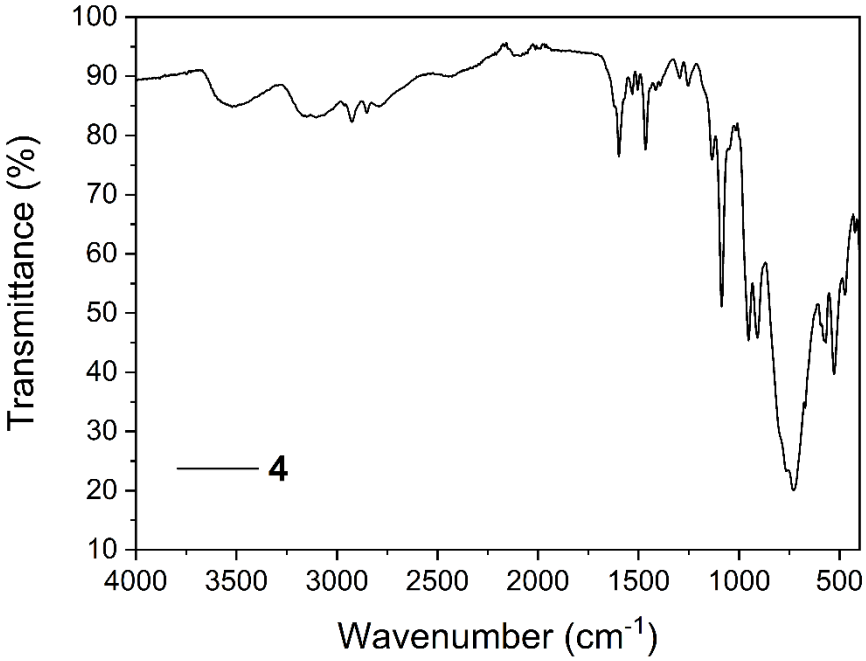

symmetric hybrid POMs **2** & **3**.

Figure S6. ATR IR spectra of **4**.

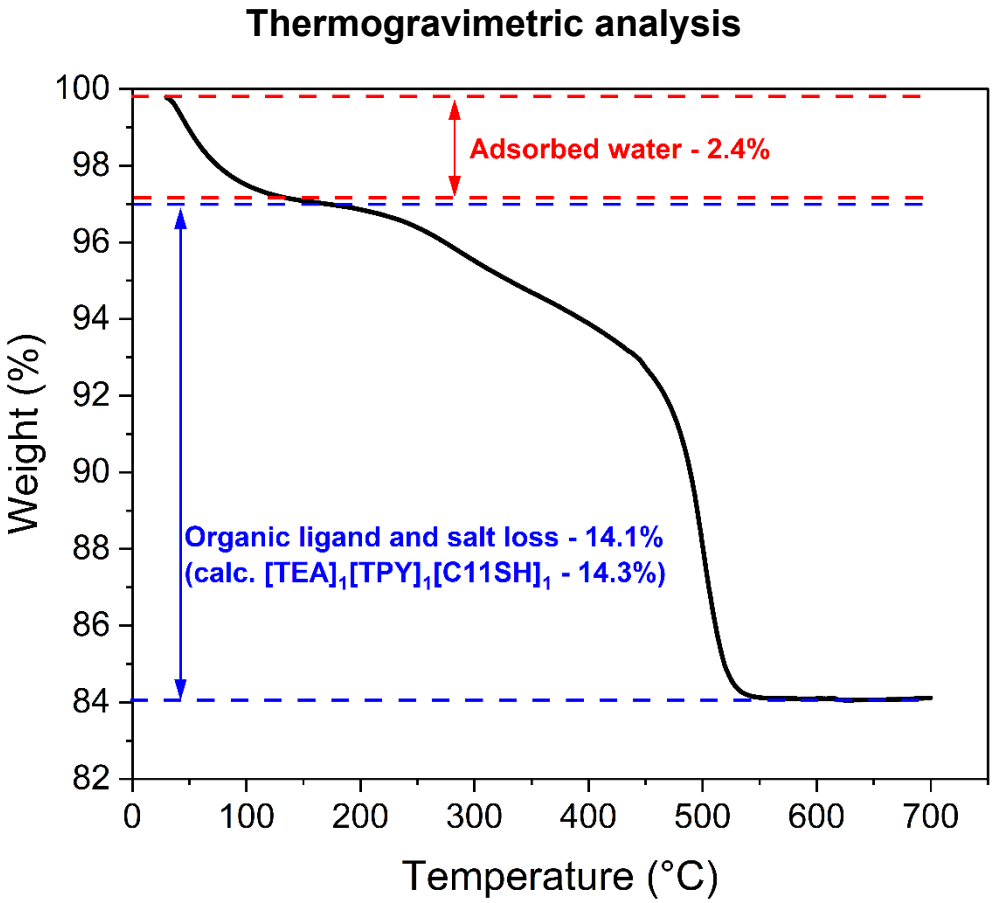

Figure S7. TGA of **4** in air showing weight loss events for adsorbed water and organic cations and ligands.

DLS Characterisation of 4

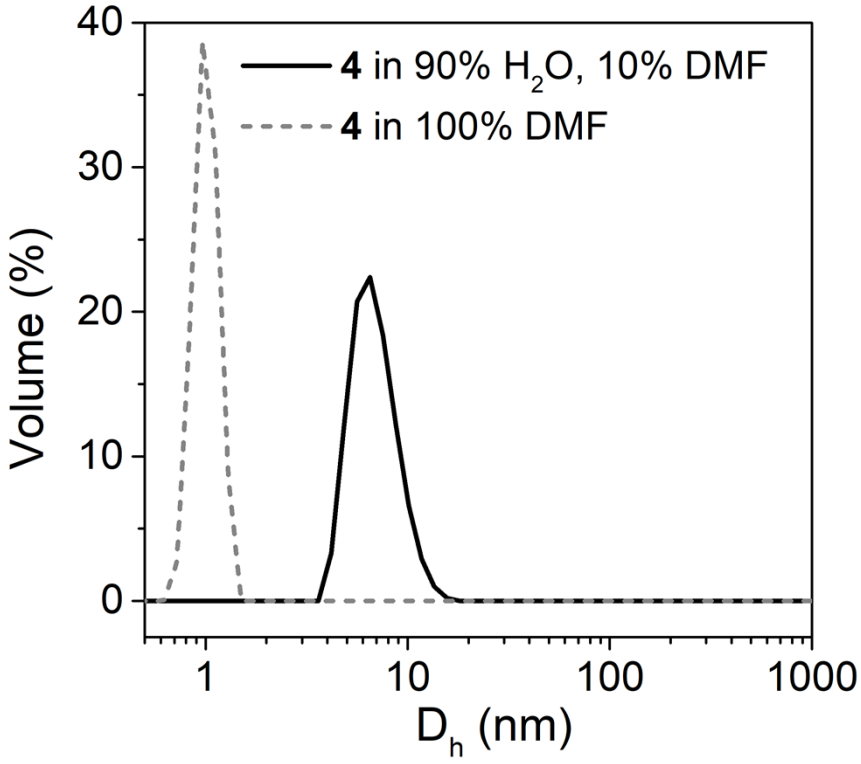

Figure S8. Particle-size distribution curve determined by DLS of: **4** (1.4 mM) in a H_2O-DMF (9:1 v/v) solution- D_h maximum at 6.5 nm (black) and **4** (1.4mM) in 100% DMF (grey dashed), D_h maximum at 1 nm (suggesting discrete molecular species only under these conditions).

Cryo-TEM of micelle solutions of 4

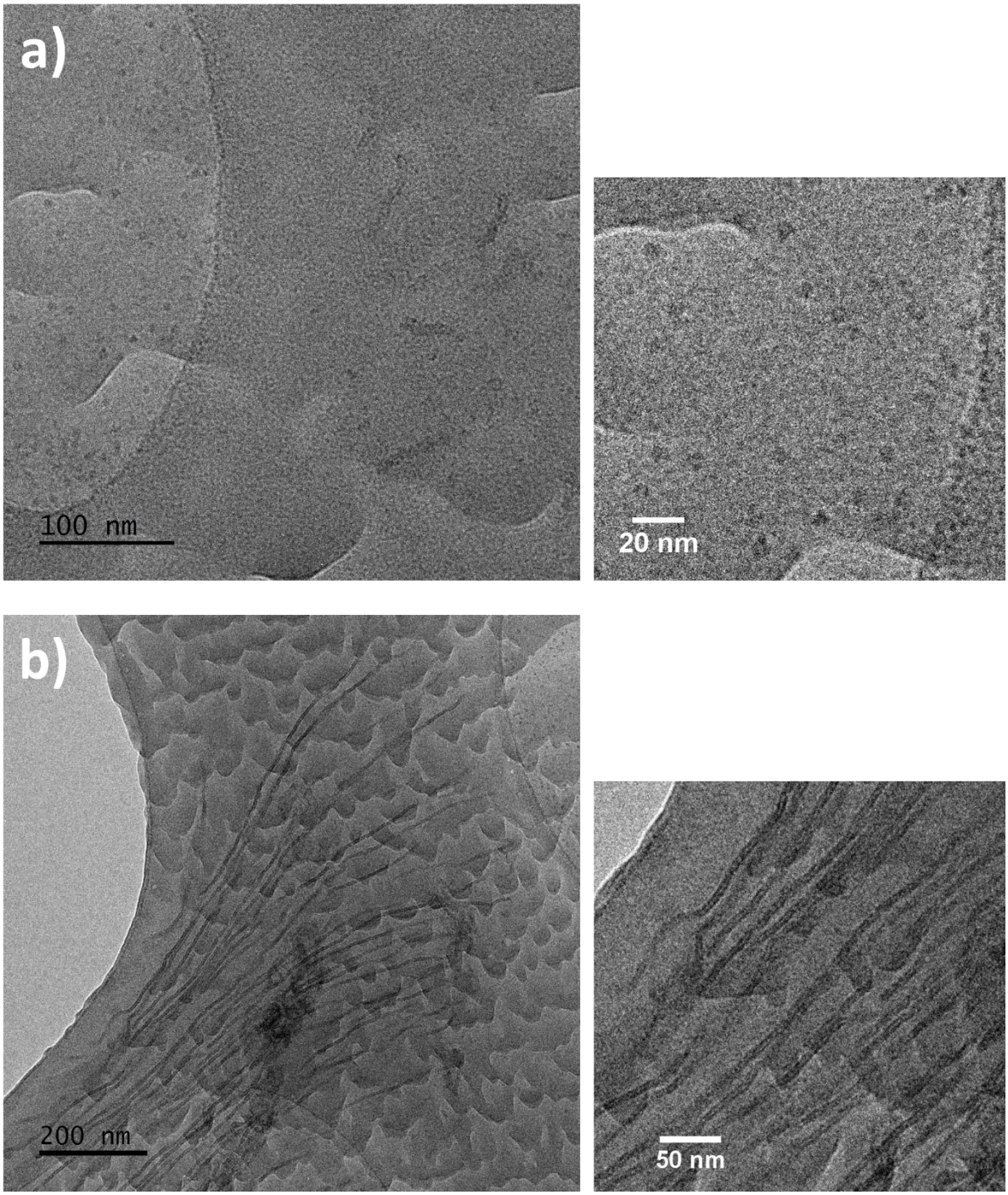

Figure S9. Cryo-TEM imaging of micellar assemblies of **4** formed in 1.4 mM water–DMF (9:1 v/v) solution. a) Sample area showing predominantly individual micellar structures; b) sample area showing long 'worm'-like assemblies formed from the aggregation of micelles.

Electrochemistry of 4 in DMF

Redox potentials vs. $Fc^+ \mid Fc^+$ (V)	I	II	III	IV
E_{red}	-0.765	-1.018	-1.447	-1.789
E_{ox}	-0.689	-0.946	-1.336	-1.695
$E_{1/2}$	**-0.727**	**-0.982**	**-1.392**	**-1.742**
ΔE_p	**0.076**	**0.072**	**0.111**	**0.094**

Table S2. Redox potentials of **4** in DMF.

DLS of 4 in 9:1 0.1M H_3PO_4/DMF electrolyte

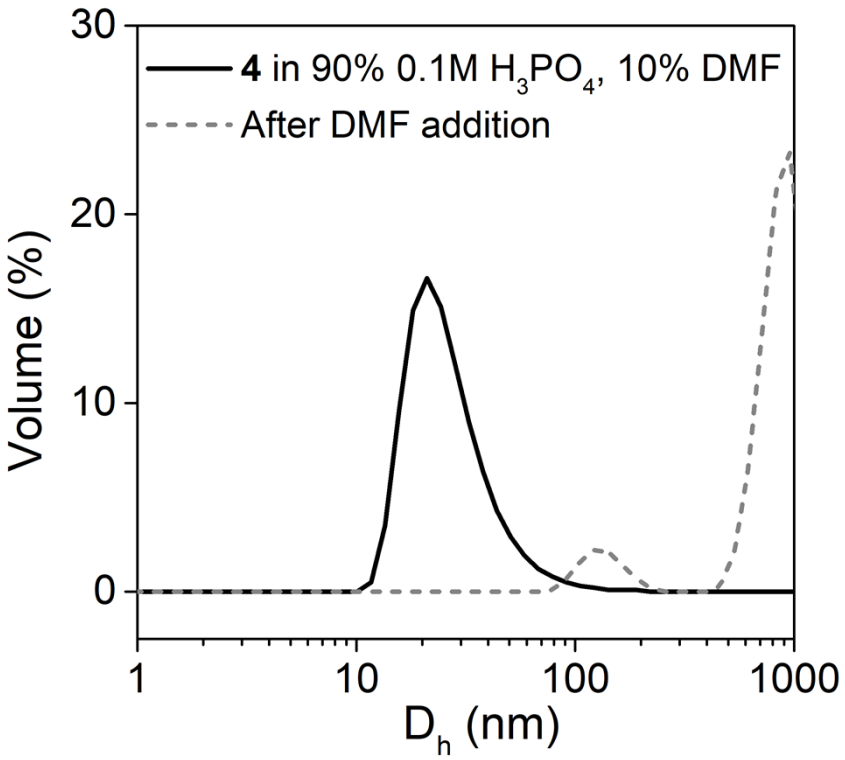

Figure S10. Particle-size distribution curves determined by DLS of the CV solution of **4** before (black), D_h maxima at 21.0 nm, and after (grey dashed) the addition of the same volume of DMF, D_h maxima at 122 nm and 955 nm.

Electrochemistry of 4@ Au electrode in 0.1 M $TBAPF_6$/DMF

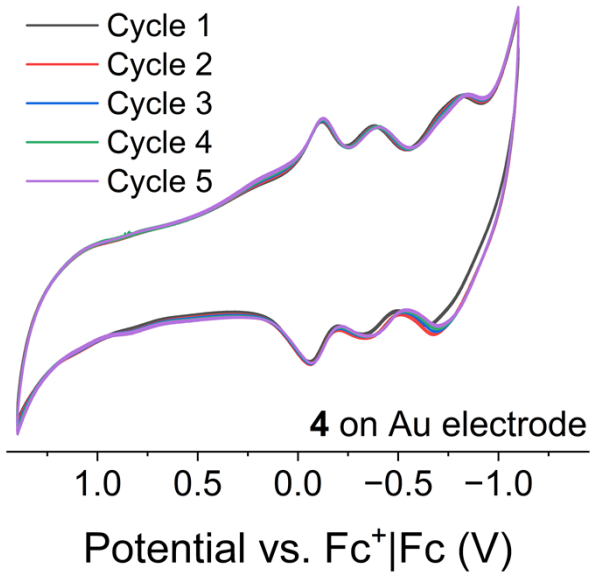

Figure S11. Cyclic voltammogram of 4 on a Au working electrode scanned at 100mV/s over 5 cycles in DMF with 0.1 M $TBAPF_6$ as electrolyte.

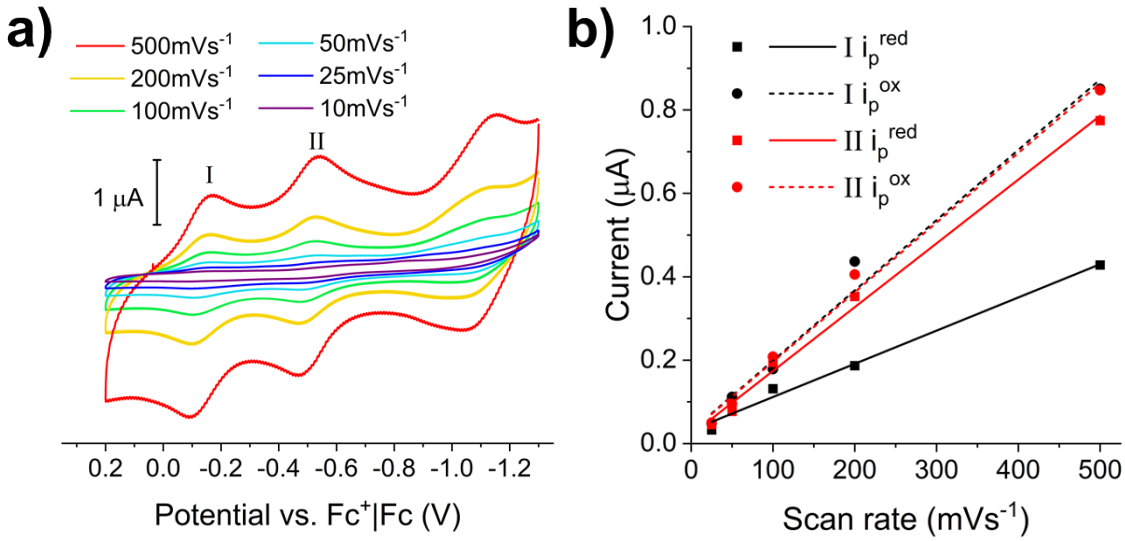

Figure S12. a) Cyclic voltammograms of **4** on a Au working electrode at different scan rates in DMF with 0.1 M $TBAPF_6$ as electrolyte; **b**) Plots of peak current vs. scan rate for the reduction and oxidation peaks of the first two redox processes of **4** showing the linear fits.

Scan rate (mVs^{-1})	Potential vs. Ag/Ag^+ (V)					
	I			II		
	E_{red}	E_{ox}	ΔE_p	E_{red}	E_{ox}	ΔE_p
500	-0.175	-0.089	**0.086**	-0.544	-0.469	**0.075**
200	-0.162	-0.100	**0.062**	-0.530	-0.468	**0.062**
100	-0.142	-0.101	**0.041**	-0.529	-0.474	**0.055**
50	-0.142	-0.102	**0.040**	-0.529	-0.474	**0.055**
25	-0.148	-0.109	**0.039**	-0.551	-0.495	**0.056**
10	-0.152	-0.089	**0.063**	-	-	-

Table S3. Peak potentials for the first and second redox processes of **4** on a Au electrode at different scan rates as seen in Fig.S10a.

Figure S13. Cyclic voltammograms of: **a**) **4** fabricated as a layer on a gold disk electrode, reduction peak used for surface coverage calculations is highlighted in the red box; **b**) **1** using a gold disk electrode over 10 cycles. Both in DMF with 0.1M $TBAPF_6$ as electrolyte. Scan rate 100 mVs^{-1}.

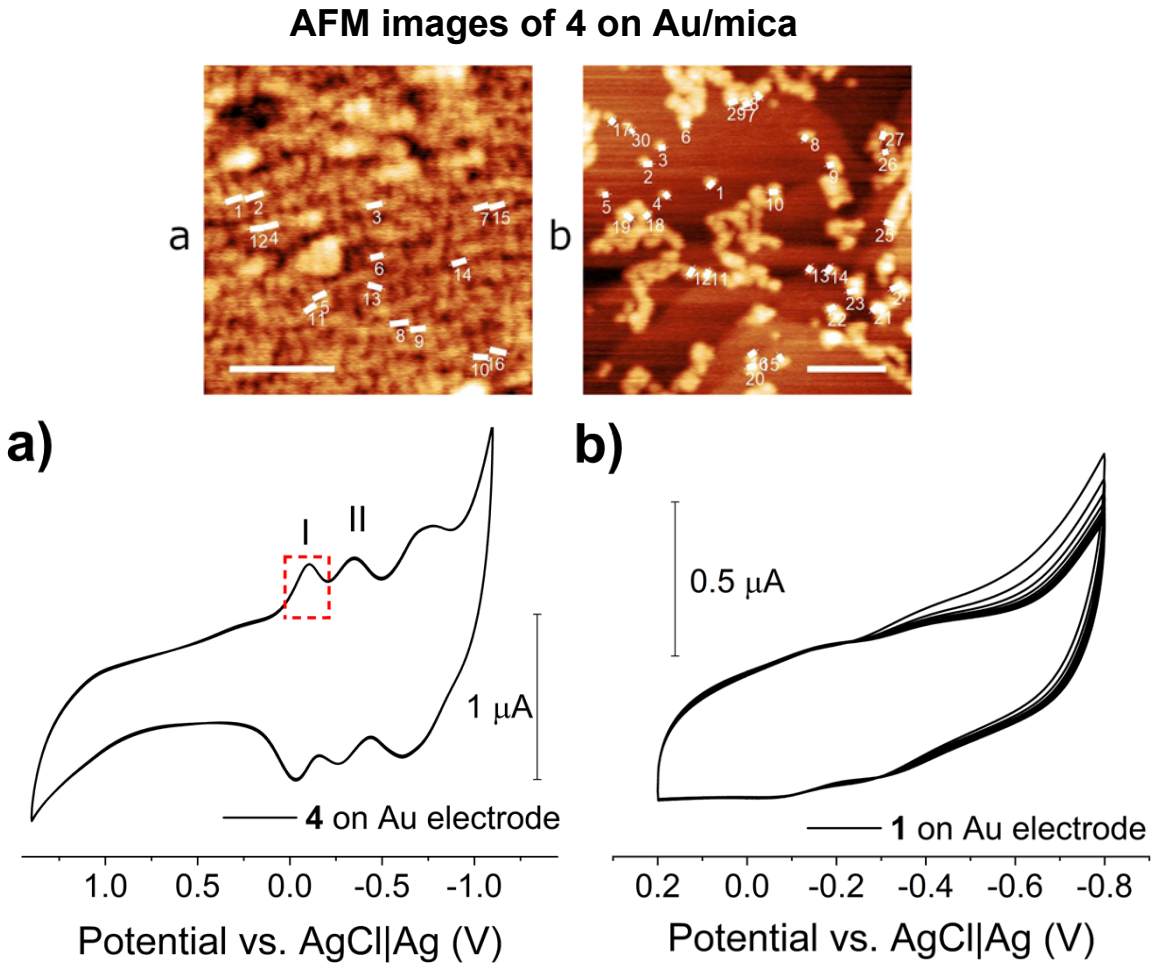

Figure S14. AFM images of **4** on Au/mica detailing the analysis of micelle diameter measurements. **a**) 16 line-profile measurements obtained from the 0.25 mM solution of **4** in DMF: average separation of 7.5± 1 nm. **b**) 60 micelle diameter measurements, across two images, (1.4 mM solution of **4** in water-DMF (9:1 v/v)) :average diameter of 5 ± 1 nm.

Figure S15. AFM images of **4** on Au/mica highlighting reconstruction of step-edge features. **a**) Molecular solution of **4** (0.25 mM solution in DMF) shows step edge curvature indicative of gold step-edge reconstruction due to thiol interaction with substrate. **b**) Micellar solution of **4** (1.4 mM solution in water-DMF (9:1 v/v)) shows straight step edges indicating weak interaction of micielles with undrlying substrate.

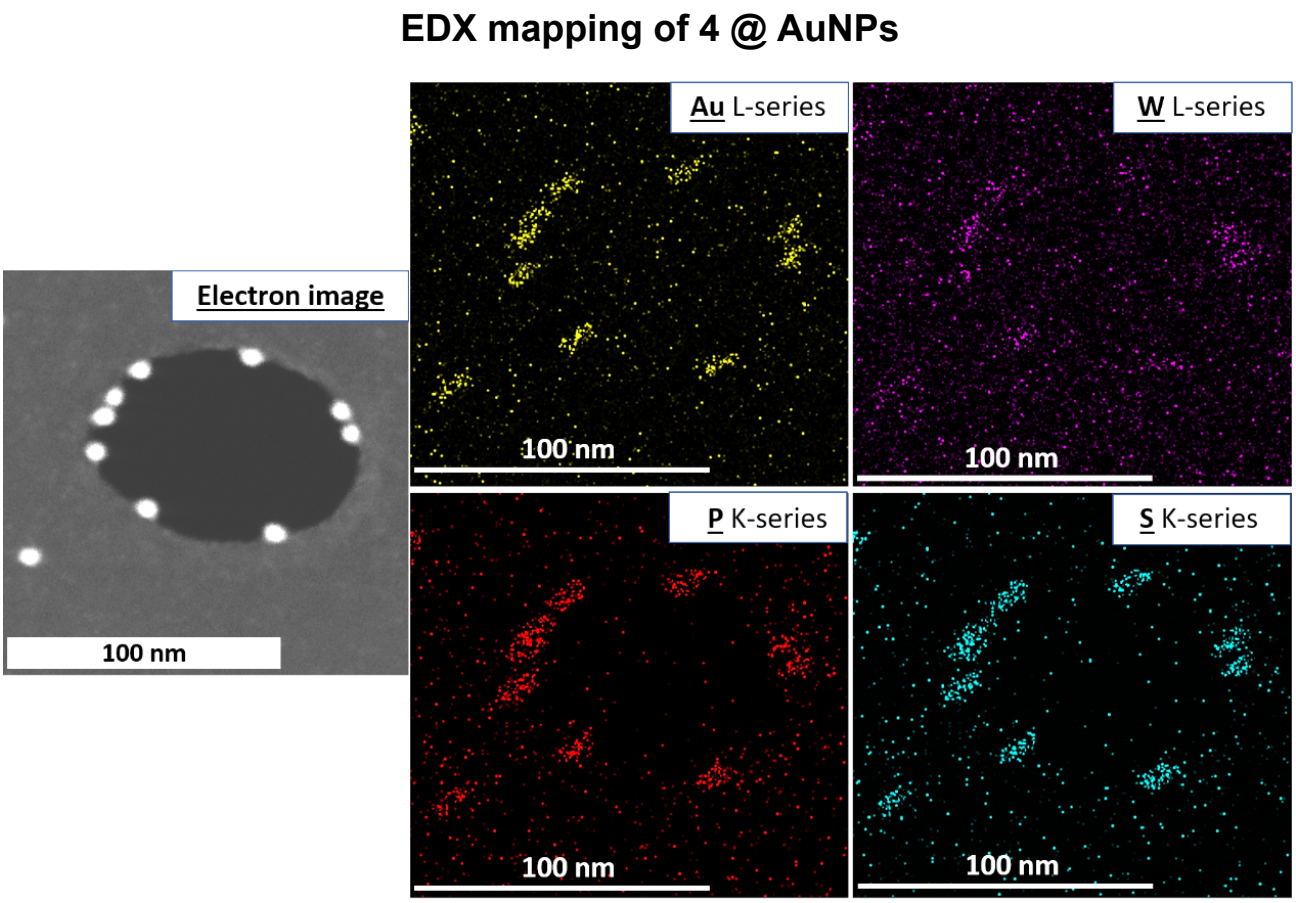

Figure S16. EDX mapping analysis of **4@AuNPs.** N.B. Quantification of EDX signals for sulfur, phosphorus and tungsten are less accurate than gold due to multiple instances of peak overlap (phosphorus and sulfur K edges lie either side of the gold M edge. The tungsten L edge lies between the copper alpha and beta K edges, the tungsten M edge cannot be used due to strong overlap with the silicon support film contaminant).

[1] G. Ing, W. A. Stewart, G. Battaglia, L. Ruiz-Perez, *PLoS ONE*, **2023**, *18*, e0285691.

[2] R. Contant, W. G. Klemperer, O. Yaghi, in *Inorg. Synth.*, John Wiley & Sons, Ltd, **1990**, 104–111.

[3] C. Graham, R. Finke, *Inorg. Chem.,* **2008**, *47*, 3679–3686.

[4] E. Hampson, J. M. Cameron, S. Amin, J. Kyo, J. A. Watts, H. Oshio, G. N. Newton, *Angew. Chem. - Int. Ed.,* **2019**, *58*, 18281–18285.

[5] C. Martin, K. Kastner, J. M. Cameron, E. Hampson, J. Alves Fernandes, E. K. Gibson, D. A. Walsh, V. Sans, G. N. Newton, *Angew Chem. Int. Ed.,* **2020**, *59*, 14331–14335.